Targeting of P-Selectin to Two Regulated Secretory Organelles in PC12 Cells

John P. Norcott, * Roberto Solari,‡ and Daniel F. Cutler*

*Medical Research Council Laboratory for Molecular Cell Biology and Department of Biochemistry and Molecular Biology, University College London, London WC1E 6BT, United Kingdom; and ‡Cell Biology Unit, Glaxo-Wellcome Medicines Research Centre, Stevenage, Hertfordshire SG1 2NY, United Kingdom

Abstract. Targeting of P-selectin to the regulated secretory organelles (RSOs) of phaeochromocytoma PC12 cells has been investigated. By expressing from cDNA a chimera composed of HRP and P-selectin, and then following HRP activity through subcellular fractionation, we have discovered that P-selectin contains signals that target HRP to the synaptic-like microvesicles (SLMV) as well as the dense-core granules (DCGs) of these cells. Mutagenesis of the chimera followed by transient expression in PC12 cells shows that at least two different sequences within the carboxy-terminal cytoplasmic tail of P-selectin are necessary, but that neither is sufficient for trafficking to the SLMV. One of these sequences is centred on the 10 amino acids of the membrane-proximal C1 exon that is also implicated in lysosomal targeting. The other sequence needed for trafficking to the SLMV includes the last four amino acids of the protein. The same series of mutations have a different effect on DCG targeting, showing that traffic to the two different RSOs depends on different features within the cytoplasmic domain of P-selectin.

NEUROENDOCRINE cells possess two kinds of organelles for regulated exocytosis; small synaptic or synaptic-like microvesicles (SLMVs)[1] and dense-core secretory granules (DCGs). The former contain only small molecules, the latter contain peptides and proteins as well. The ratio of these two regulated secretory organelles (RSOs) varies with cell type (35). Some proteins are found in the membranes of both organelles, reflecting the common requirements of exocytotic machinery (5, 36). This raises the question of how such a biorganellar distribution is attained. The itinerary of such proteins must be complex, since the biogenesis of DCGs in the TGN is very different from SLMV formation, which probably occurs in some part of the endosomal system. Moreover, the relationship between proteins that become incorporated into the two different RSOs is unclear; for example, we do not know whether membrane proteins move from one organelle to the other via recycling, nor at what point the traffic bifurcates. In addition, very little is known at the present time about the signals involved in RSO targeting of membrane proteins.

Please address all correspondence to Daniel F. Cutler, MRC Laboratory for Molecular Cell Biology and Department of Biochemistry and Molecular Biology, UCL, Gower Street, London WC1E 6BT, United Kingdom.

1. *Abbreviations used in this paper*: BB, blotting buffer; DCG, dense-core granule; HB, homogenization buffer; PAM, peptidyl-amidating monooxygenase; RSO, regulated secretory organelle; SLMV, synaptic-like microvesicle; TfnR, transferrin receptor.

Biogenesis of the SLMVs, and by implication that of small synaptic vesicles in neurons, is poorly understood. Most evidence suggests a central role for an endosomal compartment in SLMV origins. First, expression in nonneuronal cells usually leads to localization in endosomal compartments, often but not always those enriched in the transferrin receptor (4, 14, 25, 28, 29). The most parsimonious explanation for this is that the machinery necessary for a single sorting step is missing, thereby losing transfer from the endosome to the SLMV. Second, overlapping localization of endosomal markers such as rab5 (10, 15) and the transferrin receptor (TfnR; 4, 34) with SLMV membrane proteins suggests that cycling through the endosome is part of the itinerary followed by SLMV proteins. Third, considerable evidence has arisen from a detailed analysis of the trafficking of synaptophysin in PC12 cells. These rat phaeochromocytoma cells possess both RSOs (17, 18), are easily transfectable, and have become a major system for investigations into RSO biogenesis, since there are well-characterized subcellular fractionation procedures for the isolation of both granules (8, 9, 41) and vesicles (6, 8, 20, 37). Studies of SLMV biogenesis in PC12 cells have led to the conclusion that the integral membrane protein synaptophysin (or p38; 3, 22, 43, 45), found almost exclusively within SLMVs in PC12 cells (9), traffics from the *trans*-Golgi to the cell surface, and is then internalized and recycled through endosomal elements before being sorted into the SLMV (1, 9, 27, 37).

This itinerary has clear implications for the targeting sig-

nals that are likely to be present in an SLMV membrane protein.

Mutagenesis of endosomal marker proteins such as the TfnR has revealed that to attain an efficient recycling itinerary, a short cytoplasmic signal mediating recruitment to the coated pit is required (44). Removal of the cytoplasmic domain of synaptophysin causes accumulation on the plasma membrane when the truncated protein is expressed in nonneuroendocrine cells (29). In addition, it is becoming apparent that escape from the endosome–plasma membrane recycling itinerary to other destinations is a signal-mediated step (38). Together, these observations suggest that synaptophysin will require both a clathrin-coated pit internalization signal and a second sequence for subsequent sorting from the endosome to the SLMV to achieve the observed itinerary (see Fig. 10 *A*). However, this hypothesis has yet to be tested. In contrast, in the case of the integral membrane protein VAMP II (synaptobrevin II; 13), which is found in both SLMVs and DCGs in PC12 cells (5, 36), a single amphipathic helix has been demonstrated to be involved in SLMV targeting (20). Moreover, finding mutants that increase as well as decrease targeting has led to the hypothesis that VAMP II is targeted by interaction with another protein (20). Clearly, the situation is both complex and unclear.

Targeting of membrane proteins to DCGs is also poorly understood. Two proteins, peptidyl-amidating monooxygenase (PAM) and P-selectin, have been studied in some detail. PAM is a type 1 membrane protein that is found in several forms, including a soluble variant. Experiments in AtT-20 cells have shown that the granule targeting information is in the luminal portion of the molecule (31), but additional information affecting the efficiency of targeting is found in the cytoplasmic domain (33). In addition, PAM is internalized to perinuclear endosomes after reaching the cell surface, in a process that is dependent on the cytoplasmic tail of the molecule (32).

P-selectin is a type 1 membrane protein found in endothelial granules and platelets, and is involved in binding monocytes and neutrophils following its regulated appearance on the cell surface as part of the inflammatory response (24, 30). Expression in the pituicyte line AtT-20 revealed that it was targeted to the secretory granules and studies using chimeras revealed that the cytoplasmic domain was both necessary and sufficient for this targeting (12, 26). Following the fate of P-selectin by antibody-feeding experiments on transfected AtT-20 cells stimulated to secrete suggested that recycling of P-selectin to the granules in these cells can occur (42). This trafficking was dependent on sequences present in the C1 and C2 exons of the cytoplasmic domain (see Fig. 1). More recently, experiments in CHO cells have suggested the presence of a lysosomal targeting signal in the membrane-proximal C1 domain of the cytoplasmic domain (16). P-selectin therefore contains signals providing for a complex endocytic trafficking as well as for DCG targeting.

The current state of knowledge as sketched above suggests that the signals for targeting to the two RSOs found within a membrane protein present in both DCGs and SLMVs will be different. Before this work, this hypothesis has not been tested. We have made a series of chimeras between P-selectin and the enzymatically active reporter HRP (ssHRP$^{P\text{-selectin}}$) to examine targeting to RSOs in PC12 cells. The chimeras have been expressed in PC12 cells, and we have found that in addition to granule targeting, ssHRP$^{P\text{-selectin}}$ is also found in the SLMVs. We have found that two separate regions of the cytoplasmic tail are involved in SLMV targeting, and that the sequences for DCG targeting differ from those involved in targeting to the SLMV.

Materials and Methods

Cell Culture and Transfection

PC12 cells grown as described (8) were transiently transfected by electroporation (7). 1 d before transfection, the cells were plated to ~75% confluency. On the day of transfection, a 9-cm dish was trypsinized, washed once in DME plus sera, then twice in ice-cold Hebs (20 mM Hepes, pH 7.05, 137 mM NaCl, 5 mM KCl, 0.7 mM Na_2HPO_4, and 6 mM glucose). The cells were finally resuspended in 250 μl of Hebs in a 0.4-cm cuvette. 10–20 μl (~10 μg) of DNA was added, and the DNA/cell mix was given two pulses in a gene pulser (400 V, 125 μF, and infinite Ω; Bio Rad Laboratories, Hercules, CA). After 5 min, the cells were reseeded into a 9-cm dish in DME plus sera.

Constructs

ssHRP$^{P\text{-selectin}}$ in pRK34. We assembled a chimeric cDNA containing the human growth hormone signal sequence, followed by HRP and finally the transmembrane domain and cytoplasmic tail of P-selectin (Fig. 1). cDNA clones corresponding to the transmembrane domain and cytoplasmic tail of P-selectin were obtained using mRNA purified from human umbilical vein endothelial cells (using a kit from BIO 101, Inc., San Jose, CA). PolyA$^+$ RNA, purified using oligo(dT)$_{25}$ dynabeads (Dynal, Oslo, Norway), was then transcribed into cDNA using reverse transcriptase according to the manufacturer's instructions (Promega Biotech, Madison, WI). The P-selectin sequences required were then amplified from the cDNA using the following primers: 5′-GAGAACTGCAGAGTGGTCAACAG-CAACTCTA TCCAGGAAGCCCTGACT-3′ (sense) and 5′GAGAGG-ATCCGTGTTTATGG AAACCTTAAG-3′ (antisense). This PCR product was cut with BamH1 and PstI, and ligated into an HRP-pUC19 construct, where the HRP cDNA (British Biotech. Ltd., Oxford, UK) was cloned between the HindIII and EcoR1 sites in the polylinker of pUC19 that had been cut with the same two enzymes. Altogether, this generated an HRP–P-selectin fusion.

This fusion was digested with SalI/BamHI to give a 765-bp fragment containing the last half of HRP and the P-selectin transmembrane domain and cytoplasmic tail. This was ligated into pRK34 containing ssHRP KDEL (7), which had been previously digested with SalI/BglII, thus creating ssHRP$^{P\text{-selectin}}$. pRK34 was made from pGW1 (2) by taking the EcoR1/HindIII–ended polylinker from pSL1180 (Pharmacia Biotech, Piscataway, NJ) and inserting it into the EcoR1/HindIII site of pGW1. ssHRP KDEL was moved into pRK34 from pSRα (7) as a BamH1 fragment.

ssHRP P-Selectin Deletion Mutants. Deletion mutants were produced by PCR using a primer internal to HRP and primers to the cytoplasmic tail such that a STOP codon followed by an NsiI site was inserted at the required positions. These PCR products were cut with BglII and NsiI and ligated into pRK34.ssHRP$^{P\text{-selectin}}$, which had been previously cut with BglII and PstI.

Internal primer: GGCCAACGCCAACTTGCC
Cytoplasmic tail primers:
P-selectin 786: GAAGAAATGCATTTAAAATGCAGCGTTTGT
P-selectin 776: GAAGAAATGCATTTATGTAAAAACTCCATA
P-selectin 782: GAAGAAATGCATTTATCCTAGGTGGCTGTGAG-GATTCAA
P-selectin 763: GAAGAAATGCATTTAGGCTTCCTGGATAGTCAA-TGGTCC

ssHRP P-Selectin ΔC1. Primers were designed to leave a BclI site on the 3′ end of the ST region of the P-selectin tail (CCCAAGATCTT-TTTGTCTG) and a BglII site on the 5′ of the C2 region (CCTCATGAT-CACCTAGGAAC). These were ligated together and then ligated into

the BglII/PstI site of pRK34.ssHRP$^{P\text{-selectin}}$. All constructs were confirmed by sequencing.

Fractionation and Analysis

Ficoll Gradient Fractionation. The procedure used was the system described by Cramer and Cutler (8). PC12 cells were grown for 1–4 d after transfection, and DCG were labeled by incubating the cells for 2 h with 0.5 μCi/ml ^{3}H-dopamine (Amersham International, Amersham, UK) in DMEM. All operations were carried out at 4°C. Cells were washed once with 0.32 M sucrose, 10 mM Hepes, pH 7.4 (HB), scraped into 1 ml HB, and homogenized by nine passages through a ball-bearing homogenizer with a 0.012-mm clearance (made in the EMBL workshop, EMBL, Heidelberg, Germany). The cell homogenate was spun at 11,000 *g* for 5 min, and 1 ml of the supernatant (PNS) was layered on 11 ml of a 1–16% Ficoll linear gradient made in HB. The gradients were centrifuged for 45 min at 35,000 rpm in a SW40Ti rotor (Beckman Instruments, Palo Alto, CA) and fractionated in 0.5-ml fractions from the top of the tube using an Autodensi-Flow IIC (Buchler Instruments, Kansas City, MO).

Sucrose Gradient DCG Isolation. Purification of DCGs by pooling fractions containing the ^{3}H-dopamine peak from a Ficoll gradient and centrifuging to equilibrium on a 0.5–2-M sucrose gradient was carried out 4 d after transfection, as described (36).

Sucrose Gradient SLMV Isolation. Fractions 2 and 3 from a Ficoll gradient prepared as described above were layered onto an 11-ml 0.4–1.2-M linear sucrose (in 10 mM Hepes, pH 7.4) gradient. This was spun to equilibrium in a Beckman SW40Ti rotor at 25,000 rpm for 17 h, and then 0.5-ml fractions were collected and analyzed.

Glycerol Gradient SLMV Isolation. PC12 cells were assayed 2 d after transfection, since sufficient enzyme activity for easy determinations was present at this point. The procedure used was a modification of the one described by Kelly and co-workers (20). Briefly, the cells were rinsed with and then resuspended in 1 ml of buffer A (150 mM NaCl, 0.1 mM $MgCl_2$, 1 mM EGTA, and 10 mM Hepes, pH 7.4). They were then homogenized by nine passages through a ball-bearing homogenizer with a 0.012-mm clearance (EMBL workshop). The homogenate was then centrifuged in a benchtop microfuge at 14,000 *g* for 15 min. 1 ml of the resulting supernatant (S1) was loaded onto the top of an 11-ml 5–25% glycerol (in buffer A) gradient. This was centrifuged in a Beckman SW40 Ti rotor at 35 krpm for 2 h and 50 min. 0.5-ml fractions were then collected from the top using an Autodensi-Flow IIC (Buchler Instruments).

SDS-PAGE and Immunoblotting

Proteins were separated on 10% SDS-polyacrylamide slab gels, and then transferred to nitrocellulose at 300 mA for 60 min. After incubation overnight with 5% BSA, 0.2% Tween 20 in PBS (blotting buffer; BB), nitrocellulose sheets were incubated with rabbit anti-p38 (made by immunizing with the carboxy-terminal cytoplasmic domain of rat brain p38 [3] as a glutathione *S*-transferase fusion protein; kind gift from R. Kelly, University of California, San Francisco, CA and K. Buckley, Harvard Medical School, Boston, MA) primary antibodies for 1 h, washed three times in 1 h with BB, and then incubated with HRP-conjugated anti–rabbit (Jackson ImmunoResearch Laboratories, West Grove, CA) antibodies in BB for 1 h. After washing two times for 20 min with BB and once in just PBS, antigens were detected by the ECL reaction (Amersham) and exposed to autoradiographic films. For quantitative immunodetection, the signal was measured with a GS-250 Molecular Imager (Bio Rad) after exposure to a chemiluminescence-sensitive screen for 5 min.

Immunoprecipitation

6-cm dishes of PC12 cells to be immunoprecipitated were rinsed in DME lacking methionine (ICN-Flow, Oxfordshire, UK), and were then replaced in this medium supplemented with 0.25 mCi/dish of Tran^{35}S-label (ICN-Flow) for 20 min. They were then removed from the incubator, rinsed with ice-cold PBS, and lysed on ice with 0.5 ml NDET (1% NP-40, 0.6% deoxycholate, 66 mM EDTA, 10 mM Tris, pH 7.5) supplemented with PMSF (1 mM). Nuclei and debris were removed by centrifugation at 14,000 g. The supernatant was adjusted to 0.3% SDS and fixed *Staphylococcus aureus* cells were added (60 μl of a 10% suspension, Pansorbin; Calbiochem, La Jolla, CA). This suspension was rotated at 4°C for 45 min before removing the Pansorbin by centrifugation. The supernatant was taken, 2 μl rabbit anti-HRP (Dako) was added, and the sample was then incubated at 4°C overnight. Fresh Pansorbin (60 μl) was then added, and the sample was incubated at 4°C for an additional 45 min. The pellet was then collected, washed in 1 ml NDET/SDS, then 1 ml NDET/SDS/0.5 M NaCl, and finally in 1 ml PBS, and then resuspended in 50 μl sample buffer for SDS-PAGE.

HRP Assay

Fractions were assayed in triplicate. 50 μl of each fraction was added to 50 μl of the assay reagent (100 mM citrate buffer, pH 5.5, 10% Triton X-100, 0.02% H_2O_2, and 0.1% *o*-phenylene diamine [Sigma Immunochemicals, St. Louis, MO]). This was then incubated in the dark at room temperature for 1 h. The reaction was stopped by adding 50 μl of 2 M HCl, and the plates were read at 450 nm using a Bio Rad model 3550 microplate reader. Where appropriate, data obtained from glycerol gradients was corrected (multiplied by 2.5) for its effect on enzyme activity, as were data from Ficoll gradients (multiplied by 1.2).

Immunoadsorption

Immunoadsorption was carried out essentially as described (11). M-450 Dynabeads (Dynal, Oslo, Norway) coated with rat anti–mouse IgG1 were incubated with SVP-38 (monoclonal antisynaptophysin, IgG1; Sigma) or a control of mouse antimyeloperoxidase (IgG1; Dako) in PBS with 1% BSA for 16 h overnight at 4°C on a rotator, and then rinsed with PBS/BSA supplemented with 2% FCS. The beads were then mixed with pooled fractions containing the peak of HRP activity taken from a glycerol gradient. Binding of membranes to the beads occurred over 90 min at room temperature, the beads were then washed, extracted in PBS, supplemented with 1% TritonX-100, and HRP activity was determined as described above.

Antibody Feeding

After transfection, cells were plated into dishes containing glass coverslips. After 2 d, the medium was replaced with full growth medium supplemented with 1.25 μg/ml rabbit (Dako) or mouse (Sigma) anti-HRP. A 1-h incubation was followed by a brief rinse in PBS and indirect immunofluorescence was carried out using appropriate secondary antibodies (Jackson Laboratories) as described (8). Slides were viewed on an MRC-1000 confocal microscope (Bio Rad Laboratories).

Results

We initially set out to analyze the granule-targeting signals present in P-selectin. The cytoplasmic tail of this protein has been shown to contain the information responsible for targeting to granules (12), and we therefore constructed ssHRP$^{P\text{-selectin}}$ in which a reporter (HRP) replaces the luminal domain of this type 1 membrane protein (Fig. 1). HRP was used as the reporter to provide for an extremely rapid, quantitative, and convenient assay for analyzing the distribution of this chimera during subcellular fractionation. The ease of assay also makes feasible the processing of larger numbers of smaller fractions to increase the resolution of our analyses.

ssHRP$^{P\text{-selectin}}$ was transiently expressed in PC12 cells by electroporation, which leads to ~30% of the cells expressing the chimera. In an initial experiment, cells were assayed for targeting of ssHRP$^{P\text{-selectin}}$ to DCGs at various times after transfection to determine the time course of HRP activity accumulation in the DCGs. The cells to be assayed were labeled with ^{3}H-dopamine to mark the presence of the DCGs during fractionation, homogenized, and a postnuclear supernatant centrifuged on a gradient consisting of 1–16% Ficoll in isoosmotic sucrose. Samples from the gradient were collected and assayed for peroxidase activity, as well as counted for ^{3}H-dopamine (Fig. 2). The results show an accumulation with time of HRP activity in fractions 12–19, which correspond to those where

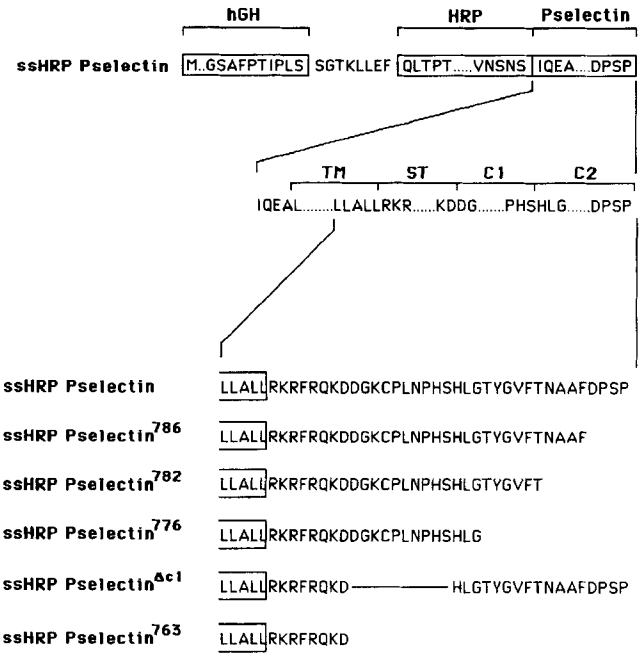

Figure 1. P-selectin chimeras. This figure shows the overall layout and relevant sequences of the chimeras used in this paper. The top line shows the main components, boxes illustrating the extent of the individual components. Sequences outside boxes were added during construction. *hGH*, human growth hormone signal sequence; *P-selectin*, transmembrane and cytoplasmic domains of P-selectin. The second line shows an expanded display of the transmembrane (*TM*) and cytoplasmic domains of P-selectin. The cytoplasmic tail includes the stop transfer (*ST*) and the C1 and C2 exons. The bottom part shows the full amino acid sequences of the cytoplasmic domains of the chimeras starting with the wild-type P-selectin tail, ssHRP$^{\text{P-selectin}}$. The carboxy-terminal end of the TM domain shown is boxed. The figure at the end of the mutant name indicates which amino acid has been changed to the stop signal (numbering is taken from the human P-selectin sequence) in that chimera. ssHRP$^{\text{P-selectinΔC1}}$ is the construct in which the C1 exon has been deleted.

^{3}H-dopamine identifies the granules (Fig. 2 *B*). As expected, ssHRP$^{\text{P-selectin}}$ therefore appears to be targeted to the granules of PC12 cells. This was confirmed by pooling the fractions of the granule peak, and centrifuging them to equilibrium on a second gradient (2), where they copurify with the dopamine (see below).

To our surprise, in cells expressing ssHRP$^{\text{P-selectin}}$, we see a second large peak toward the top of the Ficoll gradient in fractions 2 and 3 in addition to the peak of activity corresponding to the granules. This distribution is similiar to that of the SLMV marker p38/synaptophysin on this kind of gradient (8, 9). To analyze this material further, we electroporated cells with pRK34.ssHRP$^{\text{P-selectin}}$, allowed expression to occur, and then centrifuged a postnuclear supernatant on a 1–16% Ficoll gradient. The peak fractions from the top of the velocity gradient were then pooled and centrifuged to equilibrium on a sucrose gradient (reference 8 and Materials and Methods) designed for the purification of synaptic vesicles (Fig. 3). Fractions were then assayed for HRP activity and synaptophysin immunoreactivity, as determined by Western blotting. These analyses showed that the peak of HRP activity colocalized with the peak of synaptophysin (or p38) immunoreactivity, suggesting that ssHRP$^{\text{P-selectin}}$ is being targeted to the SLMVs of PC12 cells, as well as to the DCGs.

We also examined the distribution of HRP activity after ssHRP$^{\text{P-selectin}}$ expression on a completely different fractionation system that was recently used by Kelly and coworkers to examine VAMP/synaptobrevin targeting to the SLMVs of PC12 cells (reference 20 and Materials and Methods). Cells were transfected, left for 2 d, homogenized, dense material was pelleted, and a supernatant fraction (S1) was then centrifuged on a glycerol gradient (Materials and Methods). Fractions were analyzed for HRP activity and synaptophysin immunoreactivity. The results (Fig. 4) show that this glycerol gradient protocol also gave a very good correlation between p38 immunoreactivity and HRP activity, strongly suggesting that the cytoplasmic domain of P-selectin contains information capable of targeting to SLMVs of PC12 cells.

Finally, we used immunoisolation of material from the glycerol-gradient peak to confirm that the ssHRP$^{\text{P-selectin}}$ was in the same membrane boundary as p38/synaptophysin (Fig. 4, *inset*). We found that beads coated with anti-p38 could be used to isolate >90% of the enzyme activity, whereas an antibody to a non-neuroendocrine protein only pulled out ~2% of the input activity. Together, these three different approaches establish the targeting of P-selectin to SLMVs in PC12 cells.

Targeting to SLMVs of P-selectin has not been reported before, but previous analyses have largely been carried out using stable cell lines. We reasoned that the DCGs might be more stable than the SLMVs, given the endocytic origin of the latter, and that over time in a stably transfected cell line, DCG labeling might become more dominant. To investigate this, we carried out an analysis of the accumulation of HRP activity in the two different RSOs during 6 d after transfection with cDNA encoding ssHRP$^{\text{P-selectin}}$. Each day after transfection, cells were fractioned either on a 1–16% Ficoll gradient to examine the accumulation of HRP activity in DCGs, or on a glycerol gradient to examine HRP activity in SLMVs. The graph shown in Fig. 5 shows that the peak of activity in the DCGs does seem to be more stable than that in the SLMVs.

The experiments described above revealed that we have a chimera that is targeted to both RSOs in PC12 cells. This provided us with an opportunity to investigate whether signals involved in DCG and SLMV targeting are the same or different. To begin to analyze what targeting signals might be present in the chimera, we constructed a series of mutations of the cytoplasmic tail of the P-selectin chimera (Fig. 1) loosely based around the two-exon structure (23). The first exon within the tail (762–771 of the human P-selectin sequence), C1, has been shown to be involved in lysosomal targeting in CHO cells (16). We have therefore deleted this C1 domain to reveal its role in RSO targeting in PC12 cells. In addition, we constructed a deletion series through the second carboxy-proximal C2 domain.

To analyze the protein being made by this series of constructs, we electroporated the constructs into PC12 cells, allowed expression to occur, and then used a short period of metabolic radiolabeling followed by immunoprecipitation to isolate the newly synthesized material. SDS-PAGE

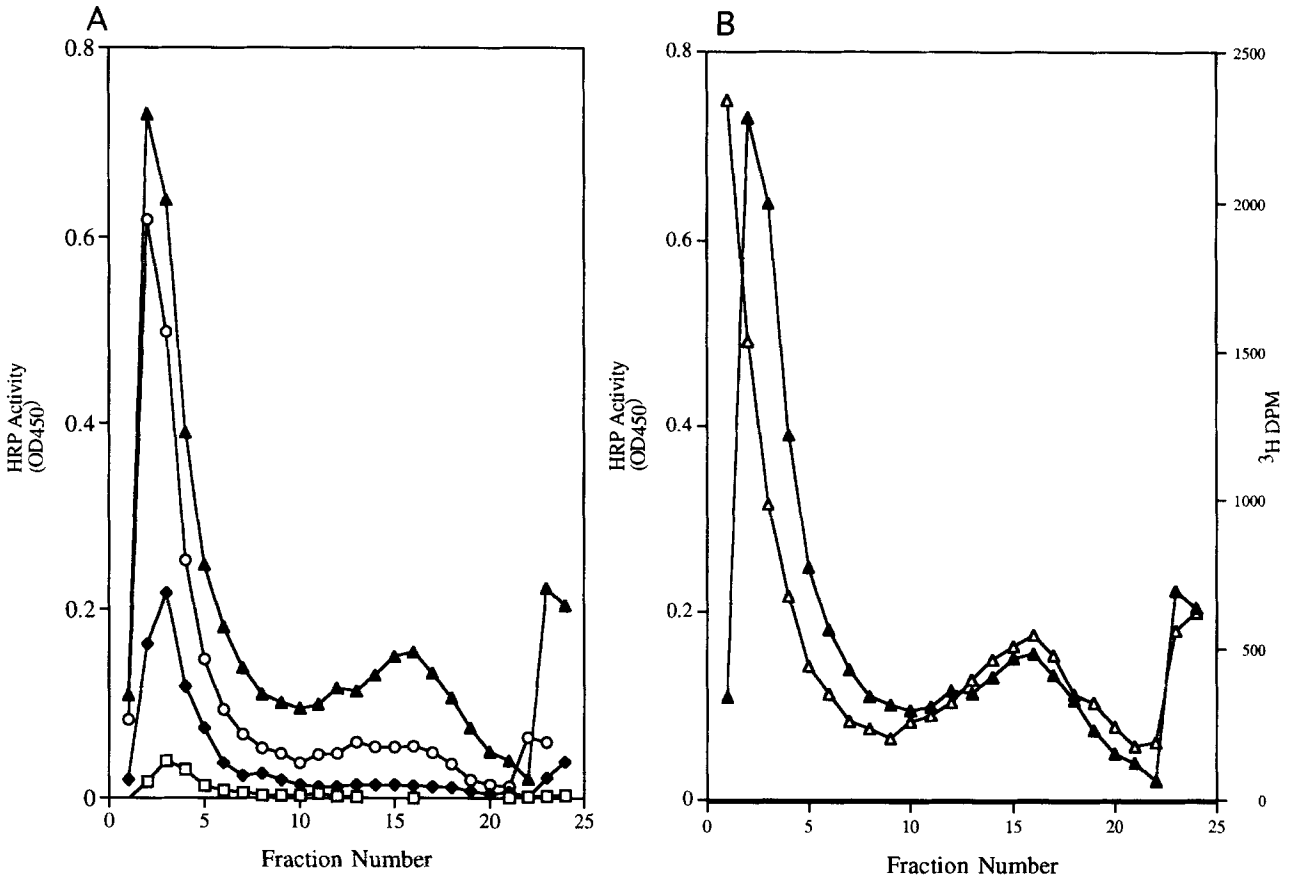

Figure 2. Distribution of ssHRP$^{P\text{-selectin}}$ on Ficoll velocity gradients at 24-h intervals after transfection. cDNA encoding ssHRP$^{P\text{-selectin}}$ was electroporated into PC12 cells that were then plated out and processed for centrifugation on 1–16% Ficoll gradients at successive 24-h intervals. Gradients were fractionated into 0.5-ml fractions, numbering from the top, and HRP activity assayed. Transfected cells were labeled with ^{3}H-dopamine before fractionation and fractions were counted. (*A*) Graph showing enzyme activity (OD_{450}) across a 1–16% Ficoll velocity gradient on 1(–□–), 2(–◆–), 3(–○–), and 4(–▲–) d after transfection. Each fraction was assayed in triplicate, and means are shown. (*B*) A comparison of HRP activity (–▲–) and ^{3}H-dopamine (–△–) labeling 4 d after transfection. Note the correspondence of the ^{3}H-dopamine peak and the peak of HRP activity in fractions 12–18. Fraction 1 is at the top of the gradient.

analysis of the immunoprecipitates demonstrates that the chimeras have the appropriate relative molecular weights (data not shown). All of the chimeras were enzymatically active.

To examine the effects of the mutations on granule targeting, cells were transfected with cDNAs encoding ssHRP$^{P\text{-selectin}}$ and the series of mutant chimeras, left for 4 d for expression to rise to levels that allow easy HRP detection during granule isolation, labeled with ^{3}H-dopamine, and fractioned on 1–16% Ficoll gradients. Fig. 6 shows the profiles of dopamine and HRP activity for all the constructs. The pattern of dopamine distribution is extremely regular, demonstrating that the fractionation procedure is very reproducible. The dopamine distribution shows a peak between fractions 12 and 19 representing the DCGs, a pellet of aggregated material, and counts at the top of the gradient representing a mixture of cell-associated dopamine that had not been taken up by the granules and dopamine released from granules during homogenization.

The HRP activity on these Ficoll gradients shows a variety of different distributions. If the activity in the granule-containing fractions (as defined by the ^{3}H-dopamine) is examined, it can be seen that ssHRP$^{P\text{-selectin}}$, ssHRP$^{P\text{-selectin786}}$, and ssHRP$^{P\text{-selectin782}}$ show significant peaks of activity. ssHRP$^{P\text{-selectin776}}$ and ssHRP$^{P\text{-selectin}\Delta C1}$ show very minor shoulders of activity where the DCGs are. ssHRP$^{P\text{-selectin763}}$ shows no significant concentration of activity in the DCG fractions. We can purify the granule fractions further by pooling and then centrifuging them on a second sucrose gradient. The data for samples containing ssHRP$^{P\text{-selectin}}$ and ssHRP$^{P\text{-selectin763}}$ treated in this way are shown in Fig. 7. The HRP activity from the DCG peak in cells transfected with ssHRP$^{P\text{-selectin}}$ remains as a single peak, in the same position as that of the dopamine on this second equilibrium gradient. The "granule peak" activity from cells transfected with ssHRP$^{P\text{-selectin763}}$, however, runs as a single peak in lighter fractions than the dopamine. The data from ssHRP$^{P\text{-selectin776}}$ and ssHRP$^{P\text{-selectin}\Delta C1}$ (not shown) reveal small but reproducible levels of activity in the granule-containing fractions on the sucrose equilibrium gradients, thus exhibiting a partial targeting phenotype.

These data suggest that the information within the cytoplasmic tail required for granule targeting is found between amino acids 763 and 782. Disdier et al. have previously shown that the granule-targeting information within the P-selectin cytoplasmic tail lies after amino acid 763, as

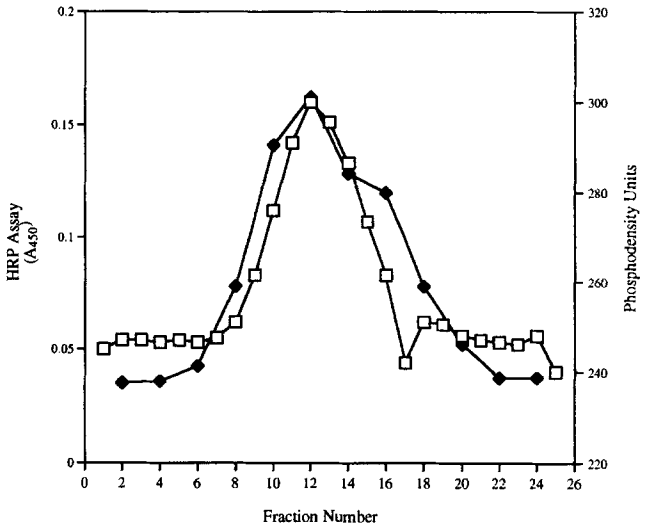

Figure 3. Codistribution of ssHRP$^{P\text{-selectin}}$ and synaptophysin on a 0.4–1.2-M sucrose gradient. Cells were transfected with pRK34.ssHRP$^{P\text{-selectin}}$, left for 2 d for HRP activity to accumulate, and then fractionated on a 1–16% Ficoll gradient. HRP activity was assayed across the gradient, and the fractions corresponding to the peak in the light fractions (2 and 3) were pooled and loaded onto a 0.4–1.2-M sucrose gradient and centrifuged to equilibrium. Fractionation was followed by assaying for HRP activity (-□-) and Western blotting for synaptophysin immunoreactivity (-◆-). Immunoreactivity is shown as phosphodensity units (*PDU*), as obtained by Phosphor-Imaging. HRP activity (OD_{450}) is shown as the mean of triplicate readings. Fraction 1 is at the top of the gradient.

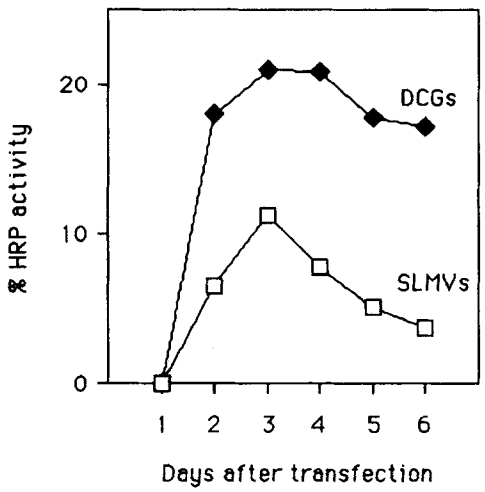

Figure 5. Time course of HRP activity in DCGs and SLMVs after transfection. Cells were transfected with pRK34.ssHRP$^{P\text{-selectin}}$ and plated out onto 12 9-cm dishes. At daily intervals, one dish was fractionated using a 1–16% Ficoll gradient, and one dish was fractionated using the glycerol gradient procedure. The HRP activity under the DCG, and SLMV peaks as a percentage of activity in the cell homogenate was calculated and is plotted against the number of days after transfection. Note that these data are not corrected for organelle recoveries during fractionation.

assayed in AtT-20 cells (12). We have established that deletion of the amino acids after 782 have little or no effect on granule targeting. Further reduction in length of the C2 domain or the removal of the C1 domain severely reduce the "granule peak."

We next examined the targeting of the chimeras to the SLMVs. We might expect to find that two regions of the cytoplasmic domain are necessary for SLMV targeting, as has been predicted for synaptophysin: an internalization signal and a signal for sorting from the endosome to the SLMV (see Fig. 10 *A*). If this is so, we would predict that deleting one of them (responsible for sorting into the SLMV from the endosome) would leave the protein in the endosome. The consequences of deleting the other might be to leave the protein accumulating on the plasma membrane. However, the actual outcome of the removal of an internalization signal on events downstream is hard to predict, since they depend on the kinetics of subsequent events as well as those of internalization. This is particu-

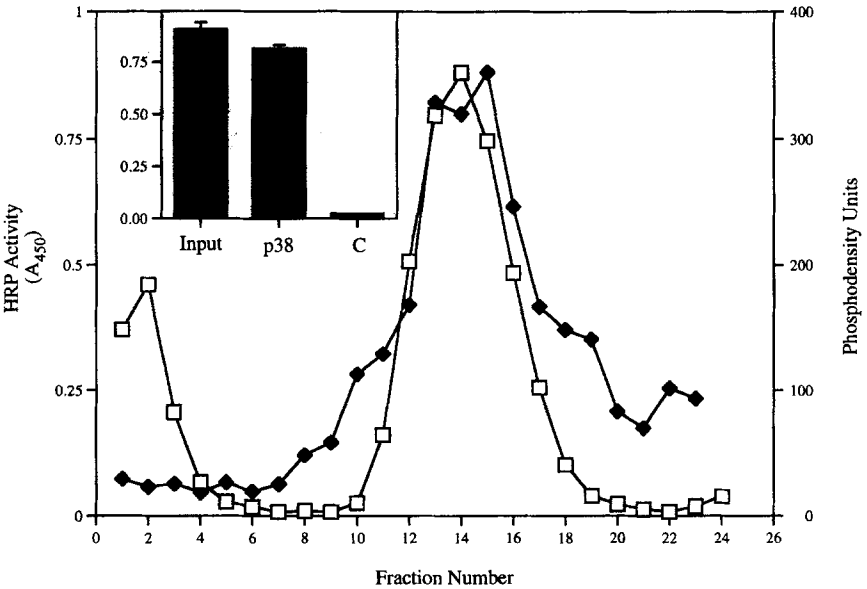

Figure 4. Codistribution of ssHRP$^{P\text{-selectin}}$ and synaptophysin on a glycerol equilibrium gradient. Cells were transfected with pRK34.ssHRP$^{P\text{-selectin}}$, left for 2 d for HRP activity to accumulate, homogenized, centrifuged, and then the S1 fraction was centrifuged on a 5–25% glycerol gradient (Materials and Methods). Samples were collected and assayed for HRP activity (-□-) and for synaptophysin immunoreactivity (-▲-). Fraction 1 is at the top of the gradient. (*Inset*) The peak fractions (12–16) from a glycerol gradient were pooled and used as input into an immunoisolation experiment as described (Materials and Methods). The graph shows HRP activity present in the input (*Input*), as well as that bound to beads coated with antisynaptophysin (*p38*) or a control antibody (*C*).

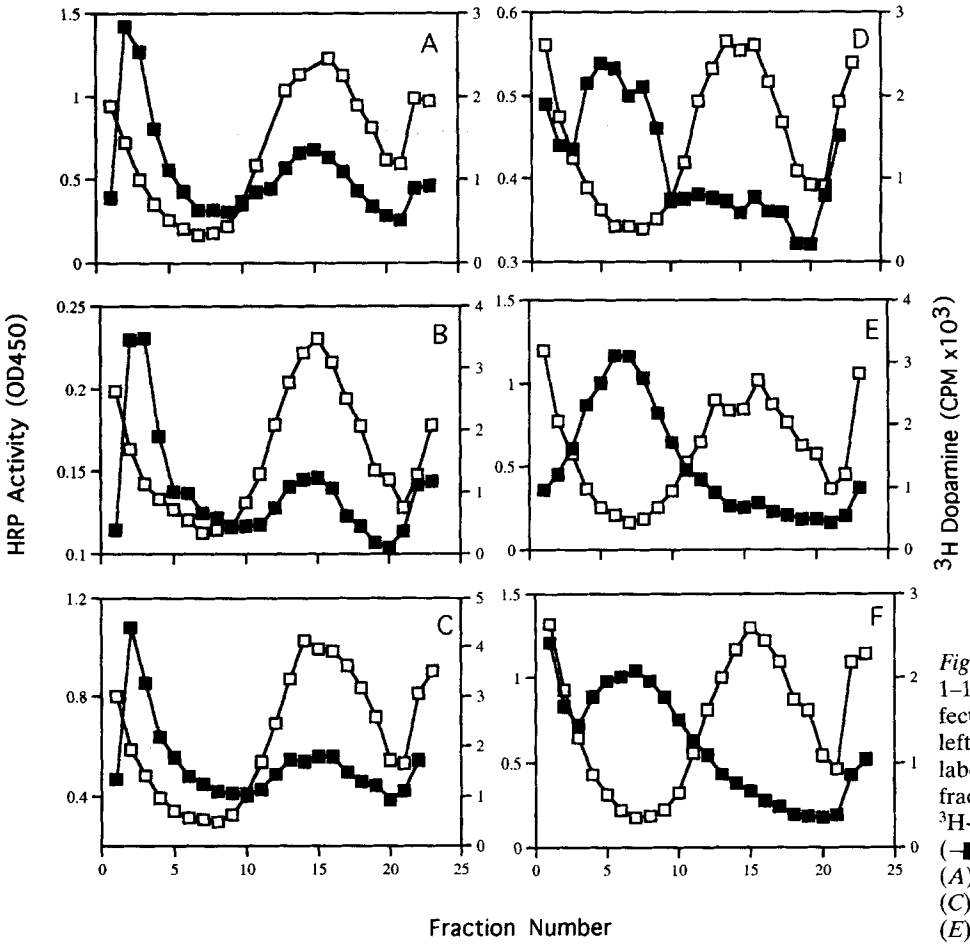

Figure 6. Distribution of chimeras on 1–16% Ficoll gradients. Cells transfected with the various chimeras were left 4 d for levels of expression to rise, labeled with ^{3}H-dopamine, and then fractionated on 1–16% Ficoll gradients. ^{3}H-Dopamine (–□–) and HRP activity (–■–) were assayed in each fraction. (*A*) ssHRP$^{P\text{-selectin}}$; (*B*) ssHRP$^{P\text{-selectin786}}$; (*C*) ssHRP$^{P\text{-selectin782}}$; (*D*) ssHRP$^{P\text{-selectin776}}$; (*E*) ssHRP$^{P\text{-selectin}\Delta C1}$; (*F*) ssHRP$^{P\text{-selectin763}}$.

larly important when a steady-state rather than a kinetic measurement of targeting is being used, as is the case in these experiments. Moreover, experiments aimed at identifying a discreet internalization signal within the cytoplasmic tail of P-selectin have not succeeded (39). The other possibility is that we might find that (as in the case of VAMP-II) a single sequence is responsible for SLMV targeting. There is no obvious sequence similarity between P-selectin and either of the other two proteins that would lead to a prediction as to which possibility is correct.

To analyze the effects of these mutations on SLMV targeting, we used the glycerol-gradient system described above. In our hands, the purity of the SLMVs obtained by pooling material from fractions 2 and 3 of the Ficoll gradients and using it in a sucrose gradient fractionation is lower than those isolated on glycerol gradients. We have therefore determined the targeting efficiency of the exogenous ssHRP$^{P\text{-selectin}}$ by comparing the enzyme activity present in the homogenate, S1 fraction, and SLMV peak of the glycerol gradient procedure. Following the example of Kelly and co-workers (20), we have also monitored the targeting efficiency of an endogenous protein (synaptophysin) in each case. This allows for variation in expression levels and in efficiency of fractionation to be monitored in each transfection/fractionation. Thus, after transfection of PC12 cells, expression was allowed to occur, and then samples were processed for analysis by glycerol gradient fractionation. We already had an indication from the Ficoll gradients shown in Fig. 6 that three of the mutants (ssHRP$^{P\text{-selectin776}}$, ssHRP$^{P\text{-selectin}\Delta C1}$, and ssHRP$^{P\text{-selectin763}}$) are unlikely to be targeted to SLMVs, since they showed no peak in fractions 2 and 3, where synaptophysin peaks. HRP activity assays of the fractions showed that all of the mutants failed to accumulate in the SLMV fractions (Table 1). No SLMV targeting whatsoever of any of the mutants was seen, despite very reproducible recoveries of synaptophysin in the SLMV peak, as assayed by quantitative immunoblotting of peak fractions and homogenates. This confirms that the material in fractions 2 and 3 on the Ficoll gradient contains a variety of organelles. We conclude that a sequence encoded at least partly within the C1 exon and a structure centered on the last four amino acids of P-selectin are both required for an itinerary that ends in targeting to SLMVs. Presumably, one of these sequences leads to inclusion in the budding SLMV, the other causing some earlier trafficking event required for delivery to the place where SLMV budding takes place. We have not yet determined whether further sequences are also involved. It is also clear from these data that granule targeting and SLMV targeting require different sequences within P-selectin.

One trivial explanation for the failure of the mutants to reach the SLMVs is that none of them enter the endocytic trafficking pathways where SLMV biogenesis is thought to occur. If, for example, they did not progress beyond early parts of the secretory pathway, then a failure to reach the

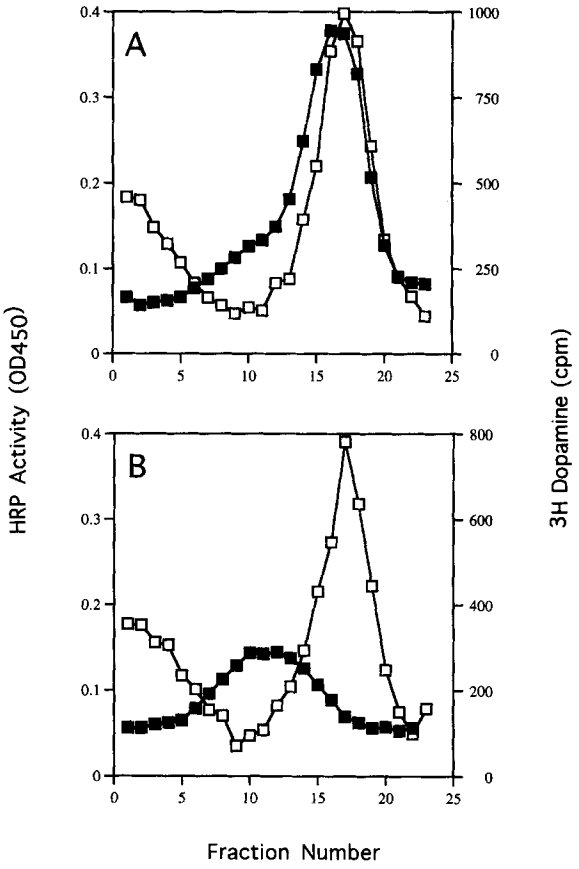

Figure 7. Distribution of ssHRP$^{P\text{-selectin}}$ and ssHRP$^{P\text{-selectin763}}$ on 0.5–1.5-M sucrose equilibrium gradients. Cells expressing ssHRP$^{P\text{-selectin}}$ (*A*) and ssHRP$^{P\text{-selectin763}}$ (*B*) were fractionated on 1–16% Ficoll gradients, and the fractions containing DCGs as defined by the ^{3}H-dopamine peak (13–17) were pooled and centrifuged to equilibrium on 0.5–2-M sucrose gradients (Materials and Methods). These gradients were collected, and fractions were assayed for ^{3}H-dopamine (-□-) and HRP activity (-■-). The Ficoll gradients from which the fractions were pooled to produce this figure are shown in Fig. 6, *A* and *F*.

SLMV would not be surprising. The fact that many of the mutants are found within DCG suggests that the mutants are capable of progressing at least to the *trans*-Golgi. It would be surprising if a chimera that reaches the *trans*-Golgi was incapable of progressing further, especially since a truncated form of P-selectin is found on the plasma membrane (12). Moreover, HRP freely passes along the secretory pathway in a number of chimeras (7, 40).

Since the key to SLMV biogenesis is thought to be entry to the endocytic pathway, we have examined the ability of the chimeras to reach the cell surface and internalize. PC12 cells were transfected so as to express the range of chimeras, and were then plated onto coverslips. The live cells growing on glass were then incubated for 1 h with antibodies (either rabbit or mouse) that recognize HRP. The rationale behind this procedure is that if the chimera reaches the cell surface, then antibody binding can occur; if internalization then follows, the antibody will be taken into endosomal elements. The distribution of the anti-HRP can then be discovered by fixing and then staining permeabilized cells with secondary antibodies coupled to a fluorophore, and using immunofluorescence microscopy. The amount of antibody used in these feeding experiments is 1.25 μg/ml, and is not detectable in untransfected cells.

The results of such experiments are summarized in Fig. 8. These representative examples show that all of the chimeras reach the cell surface. ssHRP$^{P\text{-selectin763}}$, the chimera with the shortest cytoplasmic domain, accumulates on the surface, and only internalizes to a very limited extent during the 1-h incubation period. All the other chimeras show, in addition to plasma membrane staining, intracellular localization within a variety of structures. These include large lysosomal-like punctae, as well as a more diffuse vesicular staining, often in the pericentriolar region of the cell. These results are similar to those obtained with PAM, where the internalization from the plasma membrane to pericentriolar endosomes in AtT-20 cells has been observed (32). The small round PC12 cells are not very suitable material for immunofluorescence analyses, however, and in agreement with Kelly and co-workers, we have not found it possible to analyze these structures in detail (19), beyond noting that they show similarities with both lysosomal (lgp 120) and endosomal (TfnR) markers. Apart from ssHRP$^{P\text{-selectin763}}$, only ssHRP$^{P\text{-selectin}\Delta C1}$ shows a consistently different pattern to the other mutants that are internalized. It reveals a more consistent perinuclear staining that is reminiscent of the distribution of the TfnR.

Since different anti-HRP antibodies show similar patterns, and ssHRP$^{P\text{-selectin763}}$ is not driven in from the cell surface, we believe that the internalization is not driven by the antibody, but is mediated by signal(s) present in the

Table I. Quantitation of P-Selectin Targeting to SLMVs

Chimera	HRP activity in homogenate*	HRP activity in S1 fraction*	HRP activity in SLMV peak*	HRP activity in SLMV peak (%)‡	p38 in SLMV peak (%)§
ssHRP$^{P\text{-selectin}}$	267.4 ± 6.6	81.0 ± 4.0	40.44 ± 0.4	15.1	10.1
ssHRP$^{P\text{-selectin786}}$	26.4 ± 1.4	0.0 ± 1.0	−0.4 ± 0.12	<1.0	12.4
ssHRP$^{P\text{-selectin782}}$	96.2 ± 2.4	−0.8 ± 0.6	−0.12 ± 0.12	<1.0	15.7
ssHRP$^{P\text{-selectin776}}$	209.8 ± 4	3.2 ± 0.2	−0.2 ± 0.16	<1.0	13.7
ssHRP$^{P\text{-selectin763}}$	198.2 ± 3.8	25.8 ± 2.0	−0.12 ± 0.12	<1.0	14.5
ssHRP$^{P\text{-selectin}\Delta C1}$	372.4 ± 13.4	99.0 ± 3.2	−0.36 ± 0.16	<1.0	13.0

PC12 cells transfected with cDNA encoding the indicated chimera were left for 2 d, homogenized, and then an S1 fraction was prepared. This was centrifuged on a 5–25% glycerol gradient as described (Materials and Methods) and fractionated. HRP activity in the homogenate, S1 fraction, and across the gradients were determined in triplicate for each sample. Means ± SD are shown. The SLMV peak was determined to be fractions 12–15 in this representative experiment (see Fig. 5). Homogenate and pooled peak samples were Western blotted for synaptophysin immunoreactivity.

*Total activity in assay was normalised to the starting volume.

‡Percent of homogenate activity found in the SLMV peak.

§Percent of homogenate immunoreactivity found in the SLMV peak.

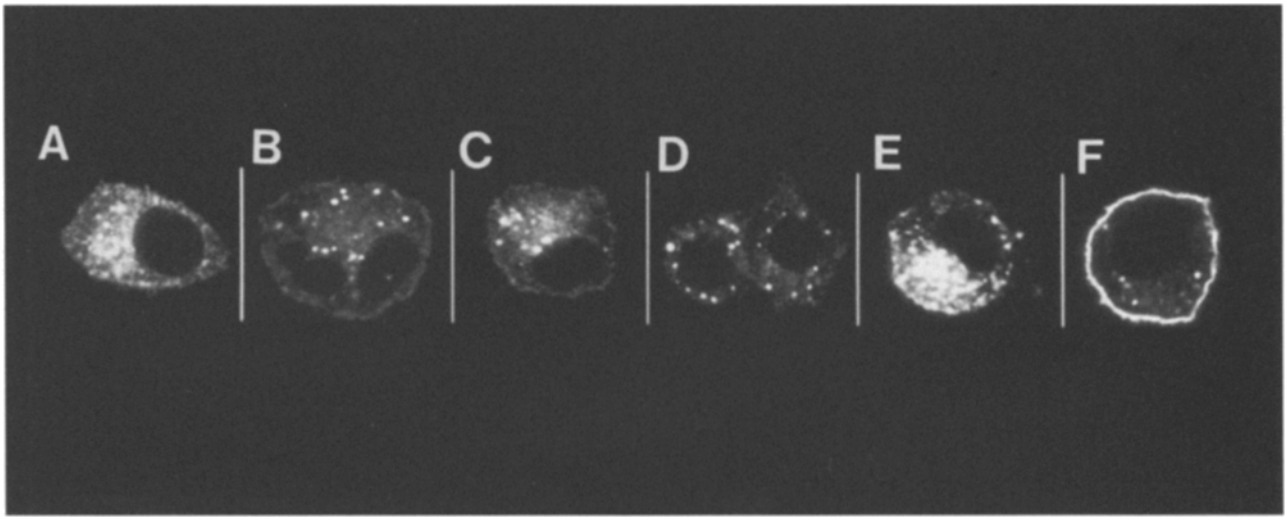

Figure 8. Distribution of P-selectin chimeras on the endocytic pathway. Cells were transfected with the P-selectin chimeras, plated onto coverslips, and subsequently incubated with anti-HRP antibodies for 1 h, as described (Materials and Methods). After fixation and permeabilization, the anti-HRP was decorated with fluoresceine-tagged secondary antibodies, and then examined on an MRC-1000 confocal microscope. (*A*) ssHRP$^{\text{P-selectin}}$; (*B*) ssHRP$^{\text{P-selectin786}}$; (*C*) ssHRP$^{\text{P-selectin782}}$; (*D*) ssHRP$^{\text{P-selectin776}}$; (*E*) ssHRP$^{\text{P-selectin}\Delta\text{C1}}$; (*F*) ssHRP$^{\text{P-selectin763}}$.

cytoplasmic domain of the chimeras. As has been previously found for full-length P-selectin (39), we find no evidence for a simple internalization signal within the tail, since we see no accumulation on the cell surface other than when most of the cytoplasmic domain has been removed. We cannot determine whether the route taken after internalization is affected by antibody binding. These data, though qualititative, suggest that chimeric molecules that are not sorted in the TGN into granules traffic to the cell surface and are then, with one exception (ssHRP$^{\text{P-selectin763}}$), capable of internalizing into at least some endosomal compartment(s), possibly including that subcompartment from which SLMV biogenesis can occur.

From the glycerol gradient data, a sequence within C1 and another centered on the last four amino acids of the cytoplasmic domain are both necessary for SLMV targeting. Models for SLMV biogenesis discussed above suggest that these two sequences might be involved in different sorting steps. If this is so, then we might see differences between the itinerary of the two mutants after reaching the cell surface. The low resolution of immunofluorescence microscopy in PC12 cells means that any differences between ssHRP$^{\text{P-selectin786}}$ and ssHRP$^{\text{P-selectin}\Delta\text{C1}}$ revealed by the antibody-feeding experiments are not clear cut, although it should be noted that neither chimera shows any evidence of accumulation on the plasma membrane. When the biochemical data in Table I are examined, however, there is some indirect evidence suggesting that the two chimeras are differentially targeted. If the fraction of activity in the S1 fraction is compared to that in the homogenate (Table I), it can be seen that ssHRP$^{\text{P-selectin786}}$ and ssHRP$^{\text{P-selectin}\Delta\text{C1}}$ show a different distribution of activity. Despite both mutants showing strong activity in the homogenate, only ssHRP$^{\text{P-selectin}\Delta\text{C1}}$ shows activity in the S1 fraction. This presumably reflects differential targeting and, together with the fluorescence, suggests that these two mutants that fail to reach the SLMVs may have different destinations after reaching the cell surface.

These results suggested that the synaptophysin-derived model of SLMV targeting was likely to be applicable to P-selectin. The strongest prediction of this model is that we should be able to find a sequence that is responsible for sorting from the TfnR-rich endosome to the SLMV. To investigate more directly whether deletion of either of these two sequences leaves the chimera in the TfnR-rich endosome, we compared the distribution of ssHRP$^{\text{P-selectin786}}$ and ssHRP$^{\text{P-selectin}\Delta\text{C1}}$ with that of a chimera comprising HRP and the signal anchor and cytoplasmic domain of the TfnR, which is targeted to the endosome (40). Of the two

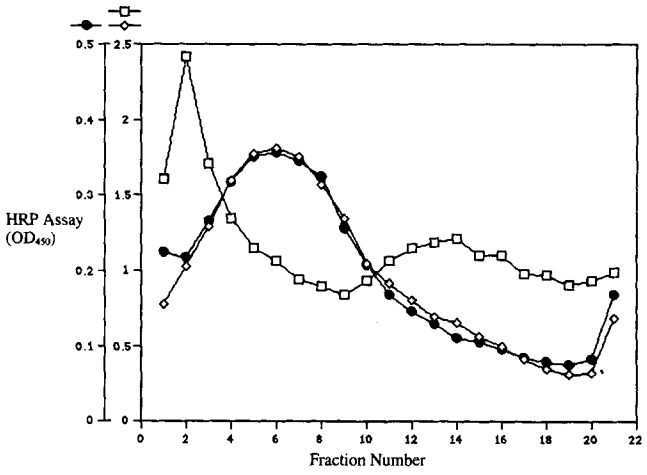

Figure 9. Distribution of ssHRP$^{\text{P-selectin786}}$, ssHRP$^{\text{P-selectin}\Delta\text{C1}}$, and TfnR-HRP activity on a Ficoll velocity gradient. 9-cm dishes of PC12 cells were transfected with cDNA encoding either ssHRP-$^{\text{P-selectin786}}$ (-□-), ssHRP$^{\text{P-selectin}\Delta\text{C1}}$ (-◇-), or TfnR-HRP(-●-), left for 4 d for HRP activity to accumulate, and postnuclear supernatants were fractionated on a 1–16% velocity gradient. HRP activity (OD_{450}) was assayed in triplicate in each fraction, and the mean is shown. Note the similarity in distribution of enzyme activity from ssHRP$^{\text{P-selectin}\Delta\text{C1}}$ and TfnR-HRP.

mutants, ssHRP$^{P\text{-selectin}\Delta C1}$ shows a distribution similar to that of the TfnR-HRP on the 1–16% Ficoll gradient system (Fig. 9). The other mutant does not show any significant colocalization with the TfnR-HRP.

Discussion

In this paper, we demonstrate that ssHRP$^{P\text{-selectin}}$ is targeted to both RSOs of PC12 cells after a transient transfection. Previous investigations of the sequences within P-selectin that are responsible for its itinerary have shown that the cytoplasmic domain is both necessary and sufficient for RSO targeting (12, 26). We are therefore confident that ssHRP$^{P\text{-selectin}}$ distribution reflects that of the full protein. Hitherto, P-selectin has been reported as being targeted to the DCGs only (12, 16, 26). The reasons for this difference may be twofold: first, we began these studies using a fractionation scheme that is deliberately designed to show both DCGs and SLMVs on one gradient, and secondly, we have used a transient expression system. Thus, the velocity gradients revealed that ssHRP$^{P\text{-selectin}}$ had a bimodal distribution reminiscent of VAMP II or synaptobrevin, which is found in both the RSOs (5, 36). Subsequent further purification of the SLMVs by two different gradient systems, one adapted from a rat brain small synaptic vesicle purification procedure (8) and one introduced by Kelly and co-workers (20), as well as immunoisolation, was used to confirm that the P-selectin was to be found in SLMVs. The physiological significance of this finding is not clear, but the differential targeting that we have revealed by mutagenesis suggests that it is not simply that any exogenous RSO membrane protein expressed in PC12 cells will end up in both RSOs as a consequence of possessing a general RSO-targeting signal. Another possible implication of our data is that a careful search of hematopoietic cells might reveal the presence of SLMV-like structures.

We suspect that the use of a transient expression system may have increased the fraction of ssHRP$^{P\text{-selectin}}$ in the SLMVs relative to the DCGs. Close inspection of the published data from expression in PC12 cells suggests that others may also have found a small fraction of this protein in the SLMVs when stable lines have been analyzed (16). Our data shown in Fig. 5 imply that in a stable line, DCGs might well become the dominant pool of this protein within RSOs. It is not clear what causes the stability of SLMVs to be lower than that of DCGs, but it may reflect a greater flow of membrane protein through the SLMV than through the DCG, resulting from a higher basal level of fusion of the former with the plasma membrane. This might reflect SLMV origins in the endosome. Moreover, the vulnerability to degradation of a protein cycling through the endosome might be exacerbated in the case of P-selectin by the presence of a lysosomal targeting signal (16).

Sorting of newly synthesised membrane proteins into DCGs probably occurs in the TGN. Published experiments (12) show that the granule targeting signal for P-selectin is located within the last 27 amino acids of the cytoplasmic domain. We have confirmed this observation, and suggest that the signal(s) location is between amino acids 763 and 782. The fact that we generate mutants (ssHRP$^{P\text{-selectin}776}$, ssHRP$^{P\text{-selectin}\Delta C1}$) that alter the efficiency of targeting rather than completely ablate it may be caused by the small number of relatively large alterations that we have made in the chimeras; we may be significantly affecting the context in which a DCG-targeting signal is operating. Alternatively, the data may suggest the presence of more than one targeting signal, which could act in concert to cause efficient targeting. These issues can be resolved by a more detailed mutagenic examination.

One important finding is that the sequences responsible for targeting to the two RSOs are different. Although it is clear that some RSO membrane proteins are differentially targeted to one or other of the two RSOs, and that therefore signals for both DCGs and SLMVs must exist, it has not before been shown that a protein with a biorganellar location can have signals for both. The only other published analysis of trafficking signals in a membrane protein that is found in both RSOs is VAMP-II. This protein turns out to have a single signal for targeting to the SLMV, which is thought to act by allowing VAMP-II to interact with an SLMV protein that does carry appropriate signals. In principle, this could extend to granule targeting as well, but granule targeting has not yet been investigated for this molecule.

One of the unresolved issues with respect to RSO targeting is the relationship between the pools of SLMV and DCG protein. In these experiments, we have found that we can make chimeras that are targeted to only one of the two RSOs. Those mutants that do reach the granules, but not the SLMVs, show no increase in DCG targeting relative to the chimera with the wild-type P-selectin sequence. This is in line with the results of the mutagenesis, which suggests that separate targeting signals exist, and therefore relatively independent targeting to the two RSOs should occur. This result is also consistent with current views of membrane trafficking, where granule biogenesis in the TGN takes place before SLMV budding in the endosome during the itinerary of a newly synthesised RSO membrane protein. This explanation also implies that there is no significant trafficking of this particular RSO protein back to the DCG from the endosome in PC12 cells. This conclusion is at variance from that of Koedam and coworkers (42), who concluded from an immunofluorescence study that recycling to granules in AtT-20 cells could occur. It is not clear whether this is cell type specific or relates to the different techniques, but we do not see any evidence of recycling to granules in the antibody-feeding experiments described above, although PC12 cells are not such a good system for light-level microscopy as AtT-20 cells. Recycling to the granule can occur in some cells, including chromaffin cells (21). It is also possible that the lysosomal-targeting signal present in P-selectin, which probably relates to the physiological role of this protein (16), operates to prevent recycling back to the granule, and that another RSO protein that lacks such a signal will behave differently. If subsequent mutagenesis enables us to generate a mutant chimera that is only targeted to the SLMVs, but not the DCGs, it will be of interest to see if SLMV targeting is increased relative to wild-type.

It has been argued above that there will be two targeting signal–dependent steps of traffic involved in the transport of proteins to SLMVs: a facilitating signal to allow efficient internalization to the endosome from the plasma

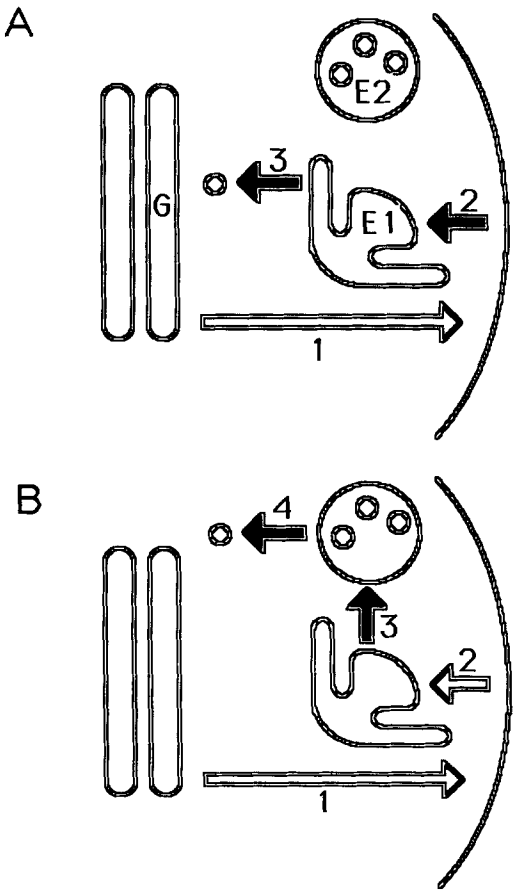

Figure 10. Models for trafficking of P-selectin in PC12 cells. This diagram illustrates the trafficking of P-Selectin from the Golgi (*G*) to the SLMV (●) via endosomal elements (*E1* and *E2*), where E1 is the TfnR-rich endosome, and E2 is some other subcompartment. Note that this diagram is simplified by ignoring that portion of the P-selectin targeted to DCGs. (*A*) A model where trafficking to the cell surface (*1*) is followed by signal-dependent internalization to E1 (*2*). A signal-dependent step (*3*) is then required for sorting into the SLMV. In this model, the sequence DPSP is required for *2*, and the C1 domain is required for step *3*. (*B*) A model where traffic to the cell surface (*1*) is followed by internalization (*2*), which may be signal dependent to TfnR-rich endosomes (*E1*). A signal-dependent step (*3*) causing sorting into a second endosomal compartment (*E2*) is followed by a second signal-dependent sorting into the SLMV (*4*). In this model, the C1 domain is required for step *3*, and the tetrapeptide sequence DPSP is required for step *4*. Filled arrows refer to the signal-dependent steps discussed above and in the main text.

membrane plus an SLMV-targeting signal that causes sorting into the the SLMV from the endosome (Fig. 10 *A*). On the other hand, VAMP II mutagenesis and expression revealed the presence of only one targeting signal (20). We interpret the results of our mutagenesis as consistent with the presence of two signals, both of which are required for arrival in the SLMV. We have no direct evidence for this, but the different intracellular locations of ssHRP$^{\text{P-selectin786}}$ and ssHRP$^{\text{P-selectin}\Delta\text{C1}}$ strongly suggests that two different signals are involved. Moreover, almost all of ssHRP$^{\text{P-selectin}\Delta\text{C1}}$ colocalizes with the TfnR-HRP chimera on Ficoll gradients, and antibody-feeding experiments show that this mutant can reach the cell surface and is then internalized to a perinuclear endosomal localization. If the SLMV arises from the TfnR-rich endosome, then this implies that the SLMV-specific targeting sequence has been removed. This is very apt, since it has been shown that in cells that lack the SLMV-specific targeting machinery, synaptophysin is found to colocalize with the TfnR (but see reference 28 for a caveat to this view).

If the C1 domain contains the SLMV-targeting signal, then the DPSP motif might be expected to be the signal for internalization from the plasma membrane. However, DPSP shows no obvious resemblance to known internalization signals (44), and its removal does not cause an accumulation on the plasma membrane, as would be revealed by the anti-HRP feeding experiments (Fig. 8). In addition, a recent analysis of endocytosis of P-selectin mutants (39) shows that removal of DPSP does not strikingly reduce internalization rates. In fact, our feeding experiments show results similar to those found by McEver and co-workers (39), who failed to identify a single simple internalization signal in P-selectin.

If the tetrapeptide DPSP is not an internalization signal, then an alternative explanation of our data may be required. The data may be explained by the C1 domain being important in targeting P-selectin away from the TfnR-positive membranes to another distribution within the endosomal system (Fig. 10 *B*), rather than from the TfnR-rich compartment to the SLMV. Given the role of the C1 domain in lysosomal targeting (16), i.e., in trafficking out of the early TfnR-positive endosome, we speculate that the C1 domain may cause targeting to a second endosomal compartment from which the SLMVs form. The DPSP motif would then be responsible for the final sorting away from this endosome to the SLMV (Fig. 10 *B*).

One of the major problems with distinguishing between these different hypotheses is that endocytic trafficking in PC12 cells is poorly understood compared with the detailed picture that is emerging from extensive work in other systems, and it is complicated by the presence both of RSOs and of the phenomenon of neuronal cell polarity. We are confident, however, that the ssHRP$^{\text{P-selectin}}$ chimeras will provide a way to unravel the complex web of post-Golgi traffic that is the itinerary of an RSO membrane protein.

This work was funded by a project grant from the Medical Research Council to D.F. Cutler.

We thank K. Buckley and R.B. Kelly for the gift of synaptophysin cDNA.We are also grateful to Lois Clift O'Grady and R.B. Kelly for advice on the immunoisolations. We thank J. Strasser for a careful reading of the manuscript.

Received for publication 15 January 1996 and in revised form 10 June 1996.

References

1. Bauerfeind, R., A. Régnier-Vigouroux, T. Flatmark, and W.B. Huttner. 1993. Selective storage of acetylcholine, but not catecholamines, in neuroendocrine synaptic-like microvesicles of early endosomal origin. *Neuron.* 11:105–121.
2. Blackstone, C.D., S.J. Moss, L.J. Martin, A.I. Levey, D.L. Price, and R.L. Huganir. 1992. Biochemical characterisation and localisation of a non-NMDA glutamate receptor in rat brain. *J. Neurochem.* 58:1118–1126.
3. Buckley, K.M.G., E. Floor, and R.B. Kelly. 1987. Cloning and sequence analysis of cDNA encoding p38, a major synaptic vesicle protein. *J. Cell Biol.* 105:2447–2456.
4. Cameron, P.L., T.C. Sudhof, R. Jahn, and P. DeCamilli. 1991. Colocaliza-

tion of synaptophysin with transferrin receptors: implications for synaptic vesicle biogenesis. *J. Cell. Biol.*115:151–164.
5. Chilcote, T.J., T. Galli, O. Mundigl, L. Edelmann, P.S. McPherson, K. Takei, and P. DeCamilli. 1995. Cellubrevin and synaptobrevins: similar subcellular localization and biochemical properties in PC12 cells. *J. Cell Biol.* 129:219–231.
6. Clift-O'Grady, L., A.D. Linstedt, A.W. Lowe, E. Grote, and R.B. Kelly. 1990. Biogenesis of synaptic vesicle-like structures in a pheochromocytoma cell line PC12. *J. Cell Biol.* 110:1693–1703.
7. Connolly, C.N., C.E. Futter, A. Gibson, C.R. Hopkins, and D.F. Cutler. 1994. Transport into and out of the Golgi complex studied by transfecting cells with cDNAs encoding horseradish peroxidase. *J. Cell Biol.* 127:641–652.
8. Cramer, L.P., and D.F. Cutler. 1992. Sorting between secretory pathways. *In* Protein Traffic: A Practical Approach. A. Magee and T. Wileman, editors. Oxford University Press. 57–85.
9. Cutler, D.F., and L.P. Cramer. 1990. Sorting during transport to the surface of PC12 cells: divergence of synaptic vesicle and secretory granule proteins. *J. Cell Biol.* 110:721–730.
10. deHoop, M.J., L.A. Huber, H. Stenmark, E. Williamson, M. Zerial, R.G. Parton, and C.G. Dotti. 1994. The involvement of the small GTP-binding protein Rab5a in neuronal endocytosis. *Neuron.* 13:11–22.
11. Desnos,C., L. Clift-O'Grady, and R.B. Kelly. 1995. Biogenesis of synaptic vesicles in vitro. *J. Cell Biol.* 130:1041–1049.
12. Disdier, M., J.H. Morrissey, R.D. Fugate, D.F. Bainton, and R.P. McEver. 1992. Cytoplasmic domain of p-selectin (CD62) contains the signal for sorting into the regulated secretory pathway. *Mol. Biol. Cell.* 3:309–321.
13. Elferink, L.A., W.S. Trimble, and R.H. Scheller. 1989. Two vesicle-associtaed membrane protein genes are differentially expressed in the rat central nervous system. *J. Biol. Chem.* 264:11061–11064.
14. Feany, M.B., A.G. Yee, M.L. Delvy, and K.M. Buckley. 1993. The synaptic vesicle proteins SV2, synaptotagmin and synaptophysin are sorted to separate cellular compartments in CHO fibroblasts. *J. Cell Biol.* 123:575–584.
15. Fischer von Mollard. G., B. Stahl, C. Walch, C. Solimena, K. Takei, L. Daniels, A. Khoklatchev, P. De Camilli, T.C. Sudhof, and R. Jahn. 1994. Localization of Rab5 to synaptic vesicles identifies endosomal intermediate in synaptic vesicle recycling pathway. *Eur. J. Cell Biol.* 65:319–326.
16. Green, S.A., H. Setiadi, R.P. McEver, and R.B. Kelly. 1994. The cytoplasmic domain of P-selectin contains a sorting determinant that mediates rapid degradation in lysosomes. *J. Cell Biol.* 124:435–448.
17. Greene, L.A., and A.S. Tischler. 1976. Establishment of a noradrenergic clonal line of rat adrenal pheochromocytoma cells which respond to nerve growth factor. *Proc. Natl. Acad. Sci. USA.* 73:2424–2428.
18. Greene, L.A., and A.S. Tischler. 1982. PC12 pheochromocytoma cultures in neurobiological research. *Adv. Cell. Neurobiol.* 3:7373–7414.
19. Grote, E., and R.B. Kelly. 1996. Endocytosis of VAMP is facilitated by a synaptic vesicle targetting signal. *J. Cell Biol.* 132:537–548.
20. Grote, E., J.C. Hao, M.K. Bennett, and R.B. Kelly. 1995. A targeting signal in VAMP regulating transport to synaptic vesicles. *Cell.* 81:581–589.
21. Hurtley, S.M. 1993. Recycling of a secretory granule membrane protein after stimulated secretion. *J.Cell. Sci.* 106:649–655.
22. Jahn, R., W.Schiebler, C. Ouimet, and P. Greengard. 1985. A 38,000-dalton membrane protein (p38) present in synaptic vesicles. *Proc. Natl. Acad. Sci. USA.* 82:4137–4141.
23. Johnston, G.I., G.A. Bliss, P.J. Newman, and R.P. McEver. 1990. Structure of the human gene encoding granule membrane protein-140, a member of the selectin family of adhesion receptors for leukocytes. *J. Biol. Chem.* 265:21381–21385.
24. Johnston, G.I., R.G. Cook, and R.P. McEver. 1989. Cloning of GMP-140, a granule membrane protein of platelets and endothelium: sequence similarity to proteins involved in cell adhesion and inflamation. *Cell.* 56:1033–1044.
25. Johnston, P.A., P.L. Cameron, H. Stukenbrok, R. Jahn, P. DeCamilli, and T.C. Südhof. 1989. Synaptophysin is targeted to similar microvesicles in CHO and PC12 cells. *EMBO (Eur. Mol. Biol. Organ.) J.* 8:2863–2872.
26. Koedam, J.A., E.M. Cramer, E. Briend, B. Furie, B.C. Furie, and D.D. Wagner. 1992. P-selectin, a granule membrane protein of platelets and endothelial cells, follows the regulated secretory pathway in AtT-20 cells. *J. Cell Biol.* 116:617–625.
27. Lah, J.J., and R.W. Burry. 1993*a*. Synaptophysin has a selective distribution in early endosomes of PC12 cells. *J. Neurocytol.* 22:92–101.
28. Leube, R.E., U. Leimer, C. Grund, W.W. Franke, N. Harth, and B. Wiedenmann. 1994. Sorting of synaptophysin into special vesicles in non-neuroendocrine epithelial cells. *J. Cell Biol.* 127:1589–1601.
29. Linstedt, A.D., and R.B. Kelly. 1991. Endocytosis of the synaptic vesicle protein, synaptophysin, requires the COOH-terminal tail. *J. Physiol. Paris.* 85:90–96.
30. McEver. R.P. 1995. Regulation of function and expression of P-selectin. *Agents and Actions.* 47(Supplement):117–119.
31. Milgram, S.L., R.C. Johnson, and R.E. Mains. 1992. Expression of individual forms of peptidylglycine α-amidating monooxygenase in AtT-20 cells: endoproteolytic processing and routing to secretory granules. *J. Cell Biol.* 117:717–728.
32. Milgram, S.L., B.A. Eipper, and R.E. Mains. 1993. COOH-terminal signals mediate the trafficking of a peptide processing enzyme in endocrine cells. *J. Cell Biol.* 121:23–36.
33. Milgram, S.L., B.A. Eipper, and R.E. Mains. 1994. Differential trafficking of soluble and integral membrane secretory granule-associated proteins. *J. Cell Biol.* 124:33–41.
34. Mundigl, O., M. Matteoli, L. Daniell, A. Thomas-Reetz, A. Metcalf, R. Jahn, and P.D. Camilli. 1993. Synaptic vesicle proteins and early endosomes in cultured hippocampal neurons: differential effects of brefeldin A in axon and dendrites. *J. Cell Biol.* 122:1207–1221.
35. Navone, F., G. Di Gioia, R. Jahn, M. Browning, P. Greengard, and P. De Camilli. 1989. Microvesicles of the neurohypophysis are biochemically related to small synaptic vesicles of presynaptic nerve terminals. *J. Cell Biol.* 109:3425–3433.
36. Papini, E., O. Rossetto, and D.F. Cutler. 1995. VAMP-2 is associated with dense-core secretory granules in PC12 neuroendocrine cells. *J. Biol. Chem.* 270:1332–1336.
37. Régnier-Vigouroux, A., S.A. Tooze, and W.B. Huttner. 1991. Newly synthesised synaptophysin is transported to synaptic-like microvesicles via constitutive secretory vesicles and the plasma membrane. *EMBO (Eur. Mol. Biol. Organ.) J.* 10:3589–3601.
38. Sandoval, I.V., and O. Bakke. 1994. Targetting of membrane proteins to endosomes and lysosomes. *Trends Cell Biol.* 4:292–297.
39. Setiadi, H., M. Disdier, S.A. Green, W.M. Canfield, and R.P. McEver. 1995. Residues throughout the cytoplasmic domain affect the internalisation efficiency of P-selectin. *J. Biol. Chem.* 270:26818–26826.
40. Stinchcombe, J.C., H. Nomoto, D.F. Cutler, and C.R. Hopkins. 1995. Identification of structures involved in anterograde and retrograde traffic between the rough endoplasmic reticulum and the Golgi apparatus. *J. Cell Biol.* 131:1387–1401.
41. Stinchcombe, J.C., and W.B. Huttner. 1994. Purification of secretory granules from PC12 cells. *In* Cell Biology: A Laboratory Handbook. Academic Press, New York. 557–566.
42. Subramanian, M., J.A. Koedam, and D.D. Wagner. 1993. Divergent fates of P- and E-selectins after their expression on the plasma membrane. *Mol. Biol. Cell.* 4:791–801.
43. Südhof, T.C., F. Lottspeich, P. Greengard, E. Mehl, and R. Jahn. 1987. A synaptic vesicle protein with a novel cytoplasmic domain and four transmembrane domains. *Science (Wash. DC).* 238:1142–1144.
44. Trowbridge, I.S., J.F. Collawn, and C.R. Hopkins. 1993. Signal-dependent membrane protein trafficking in the endocytic pathway. *Annu. Rev. Cell Biol.* 9:129–161.
45. Wiedenmann, B., and W.W. Franke. 1985. Identification and localization of synaptophysin, an integral membrane glycoprotein of M_r 38,000 characteristic of presynaptic vesicles. *Cell.* 41:1017–1028.